AMERICAN SOCIETY FOR MICROBIOLOGY | Journal of Virology®

VIRUS-CELL INTERACTIONS

Heparanase Upregulation Contributes to Porcine Reproductive and Respiratory Syndrome Virus Release

Chunhe Guo, Zhenbang Zhu, Yang Guo, Xiaoying Wang, Piao Yu, Shuqi Xiao, Yaosheng Chen, Yongchang Cao, Xiaohong Liu

State Key Laboratory of Biocontrol, School of Life Sciences, Sun Yat-sen University, Guangzhou, People's Republic of China

ABSTRACT Porcine reproductive and respiratory syndrome virus (PRRSV) continues to cause substantial economic losses to the pig industry worldwide. Heparan sulfate (HS) is used by PRRSV for initial attachment to target cells. However, the role of HS in the late phase of PRRSV infection and the mechanism of virus release from host cells remain largely unknown. In this study, we showed that PRRSV infection caused a decrease in HS expression and upregulated heparanase, the only known enzyme capable of degrading HS. We subsequently demonstrated that the NF-κB signaling pathway and cathepsin L protease were involved in regulation of PRRSV infection-induced heparanase. In addition, we found that ablation of heparanase expression using small interfering RNA duplexes increased cell surface expression of HS and suppressed PRRSV replication and release, whereas overexpression of heparanase reduced HS surface expression and enhanced PRRSV replication and release. These data suggest that PRRSV activates NF-κB and cathepsin L to upregulate and process heparanase, and then the active heparanase cleaves HS, resulting in viral release. Our findings provide new insight into the molecular mechanism of PRRSV egress from host cells, which might help us to further understand PRRSV pathogenesis.

IMPORTANCE Porcine reproductive and respiratory syndrome virus (PRRSV) causes great economic losses each year to the pig industry worldwide. The molecular mechanism of PRRSV release from host cells largely remains a mystery. In this study, we demonstrate that PRRSV activates NF-κB and cathepsin L to upregulate and process heparanase, and then the active heparanase is released to the extracellular space and exerts enzymatic activity to cleave heparan sulfate, resulting in viral release. Our findings provide new insight into the molecular mechanism of PRRSV egress from host cells, which might help us to further understand PRRSV pathogenesis.

KEYWORDS PRRSV, heparan sulfate, heparanase, viral release, porcine reproductive and respiratory syndrome virus

Received 13 April 2017 **Accepted** 2 May 2017

Accepted manuscript posted online 10 May 2017

Citation Guo C, Zhu Z, Guo Y, Wang X, Yu P, Xiao S, Chen Y, Cao Y, Liu X. 2017. Heparanase upregulation contributes to porcine reproductive and respiratory syndrome virus release. J Virol 91:e00625-17. https://doi.org/10.1128/JVI.00625-17.

Editor Julie K. Pfeiffer, University of Texas Southwestern Medical Center

Copyright © 2017 American Society for Microbiology. All Rights Reserved.

Address correspondence to Xiaohong Liu, liuxh8@mail.sysu.edu.cn.

Porcine reproductive and respiratory syndrome (PRRS) has become one of the most important diseases of intensive pig production worldwide since its emergence in the late 1980s (1, 2). This disease is characterized by respiratory disease, weight loss, and poor growth performance, as well as by late-term abortions (3). The causative agent, PRRS virus (PRRSV), is a small, enveloped, positive-sense, single-stranded RNA virus of the genus *Arterivirus*, in the family *Arteriviridae* within the order *Nidovirales* (4, 5). The PRRSV genome is approximately 15 kb in length and consists of at least 12 overlapping open reading frames (6, 7). Due to the genetic and antigenic differences, PRRSV can be divided into European genotype 1 and North American genotype 2, with Lelystad and VR-2332 as prototypical strains, respectively, which share about 60% nucleotide sequence identity (8). In 2006, highly pathogenic PRRSV (HP-PRRSV)

emerged in China, leading to a devastating fall in swine production throughout the country (9). PRRSV infection is characterized by high fever, high morbidity, and high mortality in pigs of all ages (9). As an RNA virus, PRRSV is prone to mutation, leading to genetic diversity within genotypes over time (10). Mutation and recombination are two common evolutionary mechanisms for PRRSV, which can cause enhanced fitness for survival or increased virulence (11).

As has been shown for other arteriviruses, PRRSV shows a strict cell and host tropism restriction. It preferentially infects monocytes, macrophages, and dendritic cells in swine, but there is no evidence to support its ability to infect other species (12). *In vitro*, PRRSV can be propagated in the African green monkey kidney cell line MA-104 and porcine alveolar macrophages (PAMs). Studies on the entry of the virus into the host cell have led to the identification of a number of essential virus receptors and entry mediators (13). To date, at least six cellular molecules on PAMs have been identified as putative receptors for PRRSV. They include heparan sulfate (HS), vimentin, CD151, CD169, CD163, and CD209 (14). HS is a member of the glycosaminoglycan (GAG) family of carbohydrates and is a key structural component of the extracellular matrix (ECM) and basement membrane which bind an array of growth factors, cytokines, and chemokines (15). HS is present in almost all mammalian tissues and plays a key role in ECM integrity, barrier function, and cell-ECM interactions (16). As the only known enzyme capable of degrading HS at specific intrachain sites, heparanase (HPSE) mediates the release of HS-bound cytokines, growth factors, lipoproteins, enzymes, and viruses (17). Previous studies have shown that HS expression is increased during the initial stage of herpes simplex virus 1 (HSV-1) infection to enhance viral attachment to cells. Importantly, during a productive infection, heparanase is upregulated through the NF-κB signaling pathway and translocated to the cell surface for the removal of HS to facilitate viral release (18). However, there are no reports on heparanase in PRRSV infection, and how heparanase regulates PRRSV release remains unstudied.

In this study, we attempted to investigate the mechanism of PRRSV egress from cells. We found that PRRSV caused HS degradation to allow viral exit during late stages of infection. This effect was mediated by virus-induced expression of heparanase via NF-κB. PRRSV also activated cathepsin L, a lysosomal cysteine proteinase, which can activate heparanase. Ablation of heparanase expression using small interfering RNA (siRNA) duplexes increased HS surface expression and suppressed PRRSV replication, whereas overexpression of heparanase reduced HS surface expression and enhanced PRRSV replication. Taken together, these data demonstrate that heparanase contributes to PRRSV release from cells.

RESULTS

PRRSV infection causes a decrease in HS expression on the cell surface. Previous studies have shown that HSV-1 infection upregulates heparanase for the removal of HS to allow viral exit during viral detachment (18). To determine whether PRRSV infection affects cell surface expression of HS during late stages of infection, the expression level of HS on the surface of Marc-145 cells was analyzed by flow cytometry analysis at various times or multiplicities of infection (MOIs) after infection with enhanced green fluorescent protein (EGFP)-expressing recombinant PRRSV (PRRSV-EGFP). As shown in Fig. 1A to C, HS surface expression decreased in cells infected with PRRSV-EGFP compared to that in cells that were mock infected or infected with a UV-inactivated PRRSV-EGFP at 24 and 36 h postinfection (hpi). This phenomenon was also observed at different MOIs (1 and 10) in Marc-145 cells (Fig. 1G and H). To show that the loss of HS cell surface expression correlates with PRRSV infection, we also measured the proportion of positive cells infected with PRRSV-EGFP using flow cytometry (Fig. 1D to F, I, and J). To further demonstrate that PRRSV infection causes degradation of HS, immunofluorescence microscopy was used to examine cell surface expression of HS using anti-human HS monoclonal antibody (MAb) 10E4. As shown in Fig. 1K, HS expression (red) was decreased on the surface of Marc-145 cells after PRRSV-EGFP infection (green) for

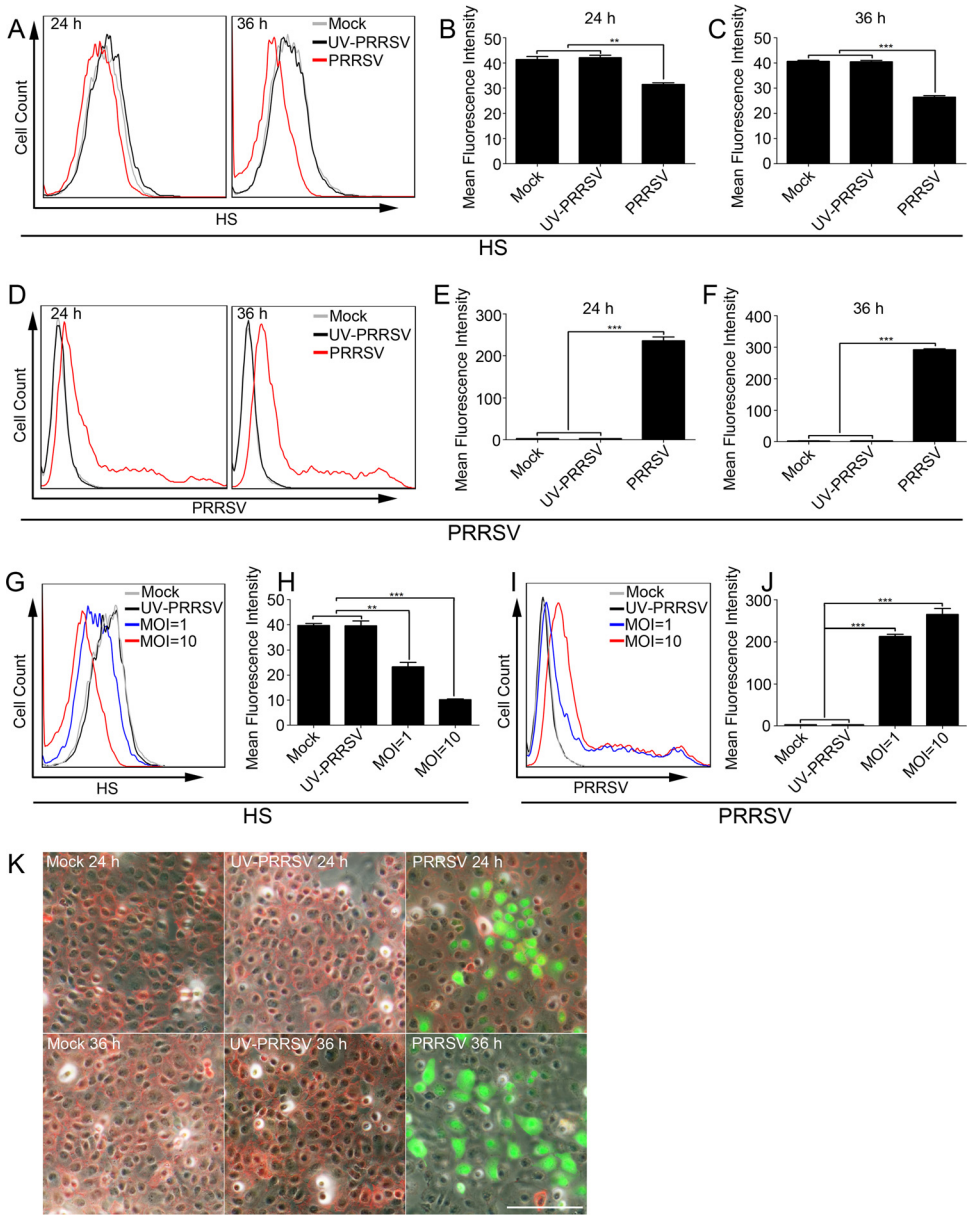

FIG 1 PRRSV infection causes a decrease in HS expression on the cell surface. (A to F) Marc-145 cells were mock infected or infected with UV-inactivated PRRSV or PRRSV-EGFP at a multiplicity of infection (MOI) of 0.1 for 24 or 36 h and then harvested to examine HS cell surface expression using anti-human HS MAb 10E4 by flow cytometry (A). Mean fluorescence intensity measurements (*x* axis, $\log_{10}$ fluorescence) were based on flow cytometry results (B and C). To show that the loss of HS correlates with PRRSV infection, viral replication was also determined by flow cytometry analysis (D to F). (G to J) Marc-145 cells were mock infected or infected with UV-inactivated PRRSV or PRRSV-EGFP at an MOI of 1 or 10 for 12 h. Surface expression of HS and PRRSV-EGFP was then detected by flow cytometry analysis. (K) Cells were mock infected or infected with UV-inactivated PRRSV or PRRSV-EGFP at an MOI of 0.1. At 24 or 36 h postinfection, the cells were fixed with 4% paraformaldehyde and analyzed by IFA using anti-human HS MAb 10E4 (red). Images were merged with bright-field images to show cell borders. Bar, 300 μm. Data are representative of the results of three independent experiments (means ± SE). Significant differences from results with the control group are indicated as follows: *, $P < 0.05$; **, $P < 0.01$; ***, $P < 0.001$.

24 or 36 h. Taken together, these data demonstrate that a dramatic decrease in HS from the cell surface was seen during late stages of PRRSV infection.

PRRSV infection upregulates heparanase. Since HS degradation was enhanced after PRRSV infection, we performed a time course analysis to determine heparanase expression in infected cells. Quantitative reverse transcription-PCR (qRT-PCR) revealed that heparanase mRNA was significantly elevated in Marc-145 cells infected with PRRSV

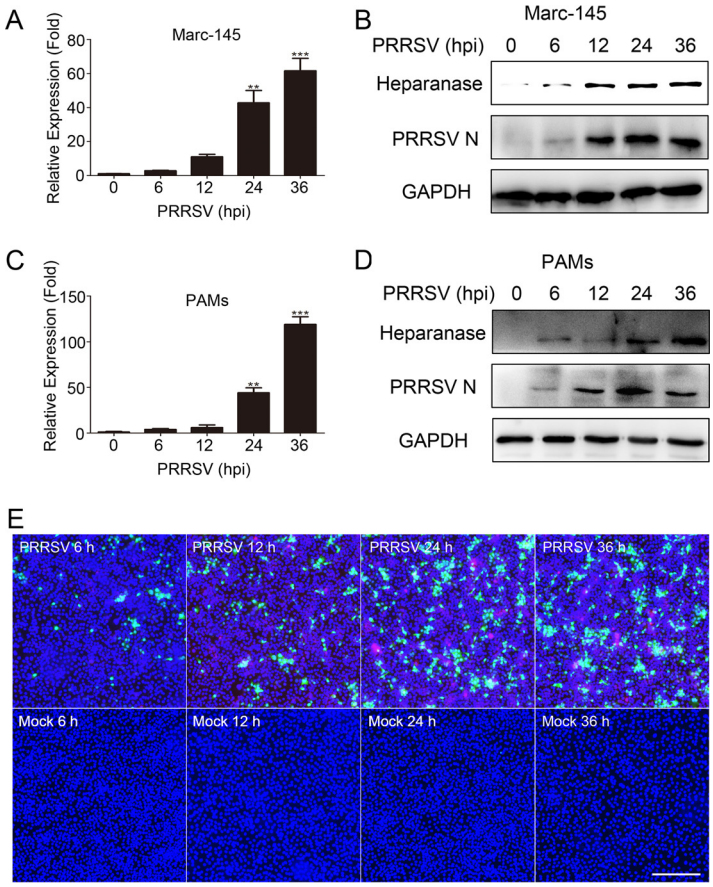

FIG 2 PRRSV infection upregulates heparanase. (A to D) Marc-145 cells or PAMs were mock infected or infected with PRRSV at an MOI of 0.1 for the indicated times. The transcript levels of heparanase were determined by qRT-PCR (A and C), and the protein levels of heparanase and PRRSV N were determined by Western blot analysis (B and D). (E) Marc-145 cells were mock infected or infected with PRRSV-EGFP at an MOI of 0.1 for the indicated times and fixed for heparanase (red) and PRRSV-EGFP (green) detection using immunofluorescence microscopy. Nucleus (blue) was stained with DAPI. Bar, 300 μm. Data are representative of the results of three independent experiments (means ± SE). Significant differences from results with the control group are indicated as follows: *, $P < 0.05$; **, $P < 0.01$; ***, $P < 0.001$.

compared to levels in cells that were mock infected at 24 and 36 hpi (Fig. 2A). Furthermore, Western blot analysis revealed that expression levels of active heparanase and PRRSV N protein were significantly upregulated in a time-dependent manner after PRRSV infection (Fig. 2B), suggesting that the increased heparanase is dependent on PRRSV infection. Similar increases in heparanase transcript levels and protein expression levels were also observed in PAMs (Fig. 2C and D), the major target cell type of PRRSV infection in pigs *in vivo*. We further showed that heparanase (Fig. 2E, red) upregulation correlated to a progressing infection (green) by using immunofluorescence microscopy. Together, these results suggest that PRRSV-infected cells upregulate heparanase expression.

Mechanism of heparanase upregulation after PRRSV infection. NF-κB is known to stimulate the expression of a number of proinflammatory cytokines as well as the catabolic enzymes (19). Inhibition of NF-κB activation by pyrrolidine dithiocarbamate leads to a significant decrease in the levels of heparanase (20), indicating that NF-κB might be an important regulator of heparanase. A number of reports have also demonstrated that PRRSV infection can activate the NF-κB signaling pathway by IκBα degradation and nuclear translocation of p65, a key subunit of NF-κB (21, 22). We therefore investigated the possible connection between NF-κB and heparanase after PRRSV infection. First, we performed a time course analysis to determine the activation

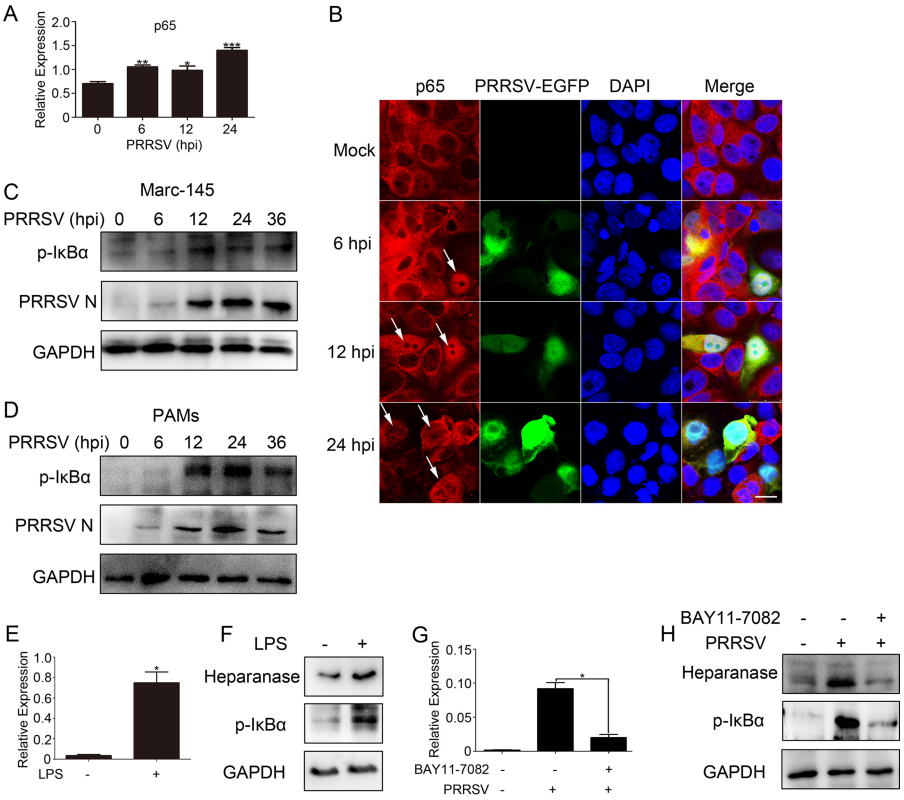

FIG 3 Mechanism of heparanase upregulation after PRRSV infection. (A) Marc-145 cells were inoculated with PRRSV (MOI of 0.1) and then harvested for qRT-PCR analysis of NF-κB p65 expression at 6, 12, and 24 hpi. (B) Cells were mock infected or infected with PRRSV-EGFP at an MOI of 0.1 for the indicated times and then fixed for immunofluorescent staining of NF-κB p65 (red). Simultaneously, PRRSV-EGFP (green) was also detected by immunofluorescence microscopy. Nucleus (blue) was stained with DAPI. Bar, 25 μm. (C and D) Marc-145 cells or PAMs were mock infected or infected with PRRSV (MOI of 0.1) for the indicated times, and cells were lysed for Western blotting to examine NF-κB p-IκBα and PRRSV N protein. (E and F) The endogenous expression of heparanase both at the mRNA level and at the protein level was determined in cells treated with or without LPS (NF-κB inducer) for 12 h. NF-κB p-IκBα was also determined by Western blotting to show the effect of LPS. (G and H) Cells were mock inoculated or inoculated with PRRSV (MOI of 0.1) in the presence or absence of BAY11-7082 (NF-κB inhibitor, 5 μM) for 24 h, and then heparanase expression was analyzed by qRT-PCR and Western blotting. Simultaneously, cells were also lysed for NF-κB p-IκBα detection to show the effect of BAY11-7082. Data are representative of the results of three independent experiments (means ± SE). Significant differences from results with the control group are indicated as follows: *, $P < 0.05$; **, $P < 0.01$; ***, $P < 0.001$.

of NF-κB in PRRSV-infected cells. As expected, the p65 mRNA was significantly increased upon PRRSV infection (Fig. 3A). Immunofluorescence microscopy results showed that in uninfected cells, p65 (Fig. 3B, red) mainly existed in cytoplasm. However, in PRRSV-EGFP-infected cells (green), nuclear accumulation of endogenous p65 was observed (Fig. 3B, arrowheads). To further confirm that PRRSV infection can activate NF-κB, IκBα phosphorylation (p-IκBα) and PRRSV N protein were also examined using antibodies against p-IκBα and PRRSV N protein. As shown in Fig. 3C and D, the levels of IκBα phosphorylation and viral N protein were significantly elevated in both PRRSV-infected Marc-145 cells (Fig. 3C) and PAMs (Fig. 3D). Thus, based on previous studies (18) and our observations, we speculated that PRRSV-induced NF-κB activation might be involved in the regulation of heparanase expression. To test this hypothesis, we then examined the effects of NF-κB inducer and inhibitor on heparanase expression. The upregulation of heparanase and of IκBα phosphorylation was observed by qRT-PCR and Western blot analysis when uninfected cells were treated with the NF-κB inducer lipopolysaccharide (LPS) (Fig. 3E and F). Conversely, we noted a decrease in heparanase expression and IκBα phosphorylation in cells treated with PRRSV and the NF-κB inhibitor BAY11-7082 (5 μM) compared to levels in cells that were treated with PRRSV

alone (Fig. 3G and H). Taken together, these data indicate that PRRSV-induced NF-κB activation is involved in the regulation of heparanase expression.

Cathepsin L upregulation after PRRSV infection contributes to the activation of heparanase. Processing and activation of heparanase occur after proteolytic processing by cathepsin L, a characteristic lysosomal cysteine proteinase of the papain superfamily of peptidases that is implicated in multiple physiological and pathological processes (23–25). To investigate whether PRRSV infection activates heparanase via cathepsin L, cathepsin L activity in Marc-145 cells was initially assessed at various times or MOIs after PRRSV infection using a Magic Red cathepsin L detection kit. Our results showed that PRRSV infection (Fig. 4A and B, green) increased the proteolytic activity of intracellular cathepsin L (red) in a time- and MOI-dependent manner, indicating that the increased activity of cathepsin L is dependent on PRRSV infection. Similar increases in cathepsin L transcript levels (Fig. 4C and D) and protein expression levels (Fig. 4E and F) were also observed upon PRRSV infection. These data show that PRRSV infection can upregulate the activity of cathepsin L protease. We next examined the effects of a cathepsin L inhibitor on heparanase expression in PRRSV-infected cells. As shown in Fig. 4G and H, the increased expression of heparanase and cathepsin L induced by PRRSV was blocked in the presence of a cathepsin L inhibitor (10 μM; Merck Millipore, MA, USA) at 24 and 36 hpi. To further demonstrate that cathepsin L upregulation upon PRRSV infection contributes to heparanase activation, the cell surface expression of HS was determined by flow cytometry in cells treated with a cathepsin L inhibitor. As expected, the cathepsin L inhibitor upregulated expression of HS at 24 and 36 hpi (Fig. 4I to K). Taking these results together, cathepsin L is involved in the activation of heparanase upregulated by PRRSV infection.

Heparanase knockdown inhibits PRRSV replication and release. To clarify the role of heparanase in PRRSV replication and release, we performed a knockdown experiment using siRNAs in Marc-145 cells. As shown in Fig. 5A and B, heparanase-specific siRNAs (S1 to S3) significantly decreased the endogenous expression of heparanase at both the mRNA level and the protein level. As expected, HS surface expression was significantly increased by knockdown of heparanase (Fig. 5C and D). Since HS is able to trap newly exiting viral progeny and block viral release during the productive period of HSV-1 infection (18), we investigated whether heparanase knockdown can inhibit PRRSV replication and egress. Marc-145 cells were transfected with a heparanase-specific siRNAs prior to PRRSV infection (MOI of 0.1). The infected cells were collected for Western blot analysis, and the supernatants were harvested for 50% tissue culture infective dose ($TCID_{50}$) and qRT-PCR analysis to determine virus titer. As shown in Fig. 5E and F, knockdown of heparanase by siRNAs S1 and S2 efficiently inhibited the level of viral N protein, and statistical analysis for measuring band intensities of viral N protein also confirmed this. Meanwhile, the amount of infectious virus production in cells transfected with siRNAs S1 and S2 was significantly decreased compared to that in cells transfected with a nontargeting control (NC) siRNA (Fig. 5G). The amount of infectious viral RNA particles released into the supernatants showed a similar pattern after heparanase knockdown by siRNA S1 and S2 (Fig. 5H). These data indicate that silencing of heparanase can suppress PRRSV replication and egress.

Heparanase overexpression enhances PRRSV replication and release. To further elucidate the role of heparanase in PRRSV replication and release, we transfected Marc-145 cells with the heparanase expression plasmid pcDNA3.1-heparanase and then infected cells with PRRSV at an MOI of 0.1 for different times. It was evident that heparanase mRNA and protein levels were enhanced in heparanase-overexpressing cells (Fig. 6A and B). In infected cells after heparanase overexpression at 24, 36, and 48 hpi, the expression level of cell surface HS was lower in cells that contained pcDNA3.1-heparanase and overexpressed heparanase than in cells that contained the pcDNA3.1 vector control (Fig. 6C to F). As expected, the protein level of PRRSV N was raised in heparanase-overexpressing cells (Fig. 6G to I). Furthermore, the viral titers and virus particles released into the cell culture supernatants were significantly increased, as

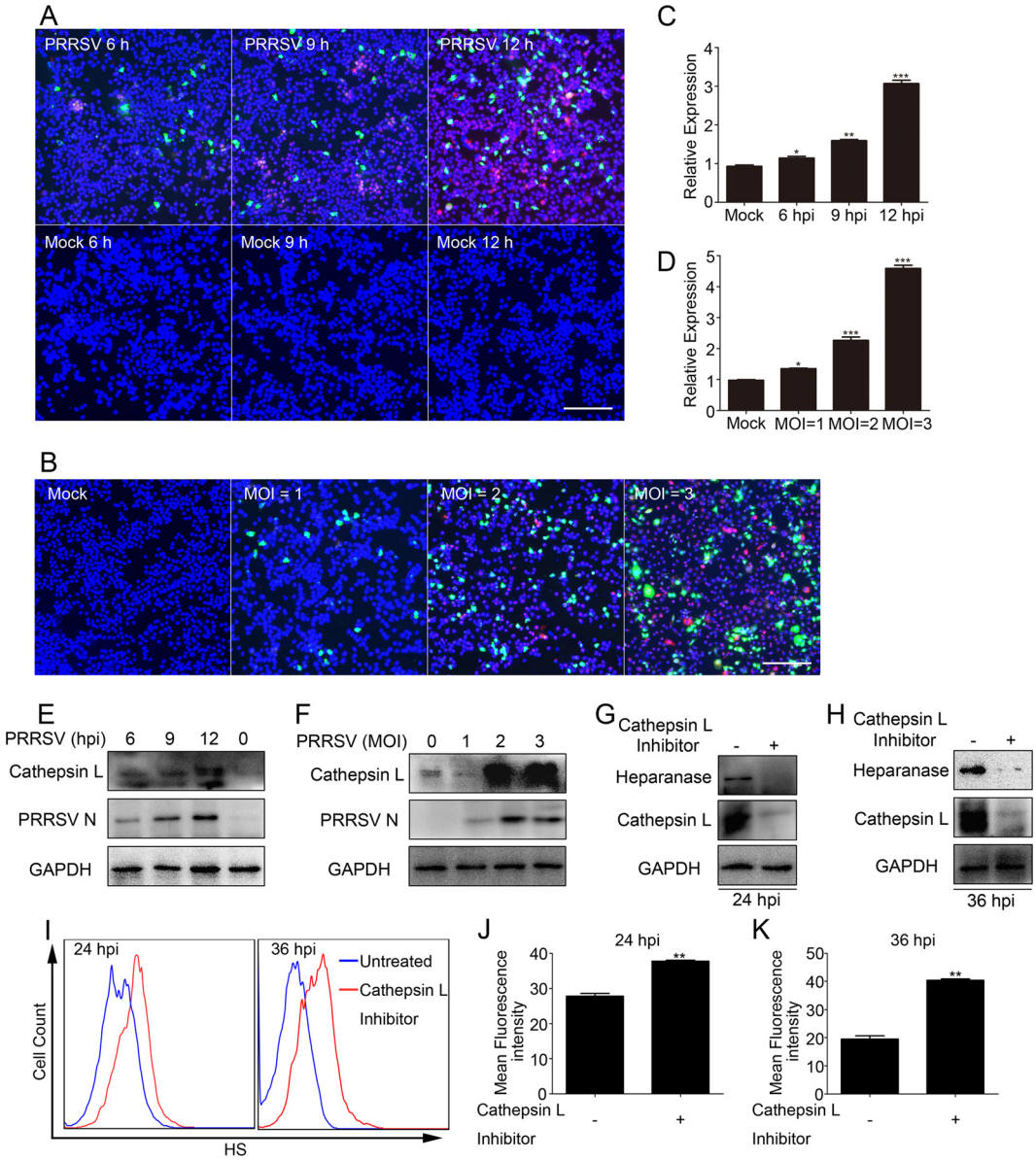

FIG 4 Cathepsin L upregulation after PRRSV infection contributes to the activation of heparanase. (A and B) Marc-145 cells were mock infected or infected with PRRSV-EGFP at an MOI of 0.1 for the indicated times or at indicated MOIs for 4 h; cathepsin L proteolytic activity (red) in cells was assessed by a Magic Red cathepsin L detection kit, and PRRSV-EGFP (green) cells were then examined by immunofluorescence microscopy. Nucleus (blue) was stained with DAPI. Bar, 300 μm. (C to F) PRRSV-infected cells were also collected to analyze cathepsin L expression using qRT-PCR (C and D), and cathepsin L and PRRSV N protein were detected by Western blot analysis (E and F). (G to K) Cells were infected with PRRSV at an MOI of 0.1 in the presence or absence of cathepsin L inhibitor (10 μM) for 24 or 36 h. The cells were harvested for heparanase and cathepsin L analysis using antibodies against heparanase and cathepsin L by Western blotting (G and H). Additionally, cells were stained for cellular surface expression of HS with anti-human HS MAb 10E4 and then determined by flow cytometry (I). Mean fluorescence intensity measurements (x axis, $\log_{10}$ fluorescence) were based on flow cytometry results (J and K). All values are representative of three independent experiments. Data are representative of the results of three independent experiments (means ± SE). Significant differences from results with the control group are indicated as follows: *, $P < 0.05$; **, $P < 0.01$; ***, $P < 0.001$.

determined by $TCID_{50}$ and qRT-PCR analysis, when heparanase was overexpressed at 24, 36, and 48 hpi (Fig. 6J and K). These results demonstrate that heparanase overexpression can upregulate PRRSV egress and replication.

A schematic model shown in Fig. 7 summarizes the main results of our study. During the productive period of infection, PRRSV activates NF-κB to promote HPSE mRNA transcription, thus increasing heparanase expression. Simultaneously, PRRSV increases the activity of cathepsin L, which subsequently processes latent heparanase into its

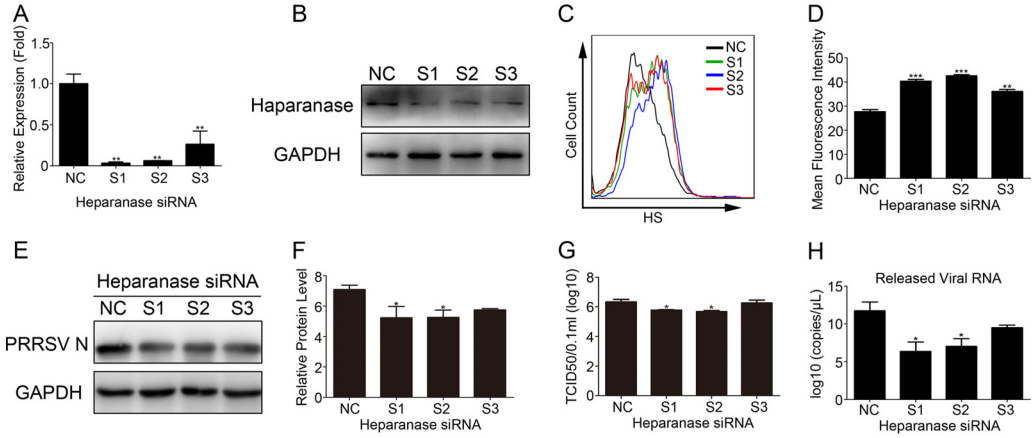

FIG 5 Heparanase knockdown inhibits PRRSV replication and release. (A and B) Marc-145 cells were transfected with heparanase-specific siRNAs at a final concentration of 50 nM for 36 h and then lysed for qRT-PCR to examine the heparanase mRNA level (A) or for Western blotting to examine heparanase protein levels (B). (C to F) Cells were transfected with heparanase-specific siRNAs for 36 h, followed by infection with PRRSV at an MOI of 0.1. At 24 hpi, cells were collected for flow cytometry analysis of HS cell surface expression using anti-human HS MAb 10E4 (C) or for PRRSV N protein detection by Western blot analysis (E). Mean fluorescence intensity measurements were based on flow cytometry results (D). The level of viral N protein was quantified by measuring band intensities and normalized with respect to the amount of GAPDH (F). (G and H) Simultaneously, the supernatants were harvested to measure viral titers (G) and extracellular viral particles (H) using $TCID_{50}$ and qRT-PCR analysis, respectively. Data are representative of the results of three independent experiments (means ± SE). Significant differences from results with the control group are indicated as follows: *, $P < 0.05$; **, $P < 0.01$; ***, $P < 0.001$.

enzymatically active form. The active heparanase is then released to the extracellular space and exerts enzymatic activity to cleave HS of the ECM, resulting in the release of virus attached to fragments of ECM-resident HS.

DISCUSSION

HS is a glycosaminoglycan (GAG) that is present in almost all mammalian tissues on cell surfaces and in the extracellular matrix (17, 26, 27). It plays a key role in ECM integrity, barrier function, and cell-ECM interactions and is used by many viruses for initial attachment to target cells. To date, several important PRRSV receptors, including HS, CD163, CD169, CD151, CD209, and vimentin, have been suggested. HS was identified as a possible mediator for PRRSV attachment and entry. Previous studies have shown that HS expression is increased during the initial stage of HSV-1 infection to enhance viral attachment to cells (18). However, during a productive infection, heparanase is upregulated through the NF-κB signaling pathway and translocated to the cell surface for the removal of HS to facilitate viral release (18). In this study, we attempted to investigate the mechanism of PRRSV egress from cells. We found that PRRSV infection induced heparanase expression, which was then translocated to the cell surface, cleaving HS to allow viral egress (Fig. 7). Ablation of heparanase expression using small interfering RNA duplexes increased cell surface expression of HS and suppressed PRRSV replication and release (Fig. 5), whereas overexpression of heparanase reduced HS surface expression and enhanced PRRSV replication and release (Fig. 6). These data indicate that the upregulation of heparanase is likely a host response to infection that the virus takes advantage of to avoid reattachment to HS and reentry into parent cells, thus increasing viral release and spread.

Since heparanase overexpression increases viral release, the amount of virus particles released in the cell culture supernatants is enhanced, leading to increased virus particle production (Fig. 6J and K). The released viral particles can spread and directly infect adjacent cells, resulting in enhanced viral replication. Taking these observations together, heparanase overexpression is capable of increasing viral N protein levels. In the experiment shown in Fig. 1K, infected and uninfected cells have decreased levels of HS at 36 hpi (PRRSV 36 h panel), indicating that PRRSV can directly or indirectly cause a decrease in HS levels. Although the infectious viral titer is moderately affected (Fig. 5G

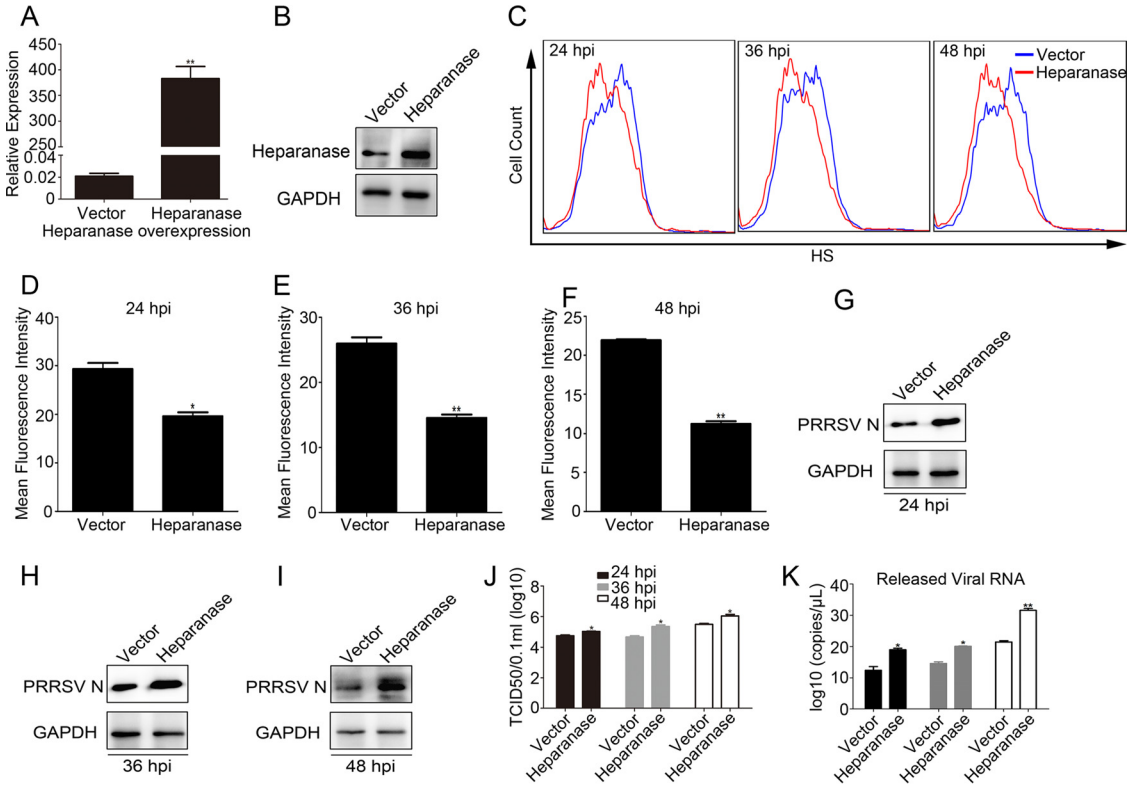

FIG 6 Heparanase overexpression enhances PRRSV replication and release. (A and B) Marc-145 cells were transfected with the heparanase expression plasmid pcDNA3.1-heparanase or the pcDNA3.1 control, and cells were harvested 36 h later to determine the transcript (A) and protein (B) levels of heparanase by qRT-PCR and Western blot analysis. (C to I) Cells were transfected with the heparanase expression plasmid pcDNA3.1-heparanase or the pcDNA3.1 control for 36 h and then infected with PRRSV (MOI of 0.1). At 24, 36, and 48 hpi, cell surface expression levels of HS (C) and PRRSV N protein (G to I) were determined by flow cytometry and Western blotting, respectively. Mean fluorescence intensity measurements (*x* axis, $\log_{10}$ fluorescence) were based on flow cytometry results (D to F). (J and K) Simultaneously, the supernatants were harvested to measure viral titers (J) and extracellular viral particles (K) using $TCID_{50}$ and qRT-PCR analysis, respectively, at the indicated time points. Data are representative of the results of three independent experiments (means ± SE). Significant differences from results with the control group are indicated as follows: *, $P < 0.05$; **, $P < 0.01$; ***, $P < 0.001$.

and 6J), total levels of virus are more severely impaired following heparanase knockdown or overexpression (Fig. 5H and 6K). One possible reason is that silencing or overexpression of heparanase may mainly regulate the amounts of released viral RNA since heparanase is involved in viral release. However, the exact molecular mechanism remains unclear. Further research is required to explore it in the future.

Heparanase is the only known mammalian endoglycosidase capable of cleaving HS (28–30). It is produced as a latent 65-kDa proenzyme that is processed and activated by cathepsin L, yielding an enzymatically active heterodimer composed of 8- and 50-kDa subunits (31). Under physiological conditions, heparanase is expressed at high levels only in a few tissues while under specific pathological conditions, it is upregulated and highly affects multiple biological processes, indicating that it might be recognized as a negative prognostic marker (16). Heparanase is involved in many different pathological scenarios, such as inflammatory diseases, angiogenesis, cancer, and metastasis (16). Therefore, heparanase has attracted considerable attention as a promising target for innovative pharmacological applications. In this study, our results demonstrated that PRRSV activated NF-κB and cathepsin L to upregulate and process heparanase (Fig. 3 and 4), which is involved in viral release, indicating that heparanase might be a unique therapeutic target against PRRSV infection. Further research should be undertaken to clarify the molecular mechanism by which PRRSV activates cathepsin L.

Previous studies have shown that PRRSV infection inhibits NF-κB activation (32, 33). However, in this study, we found that PRRSV infection activated NF-κB and cathepsin

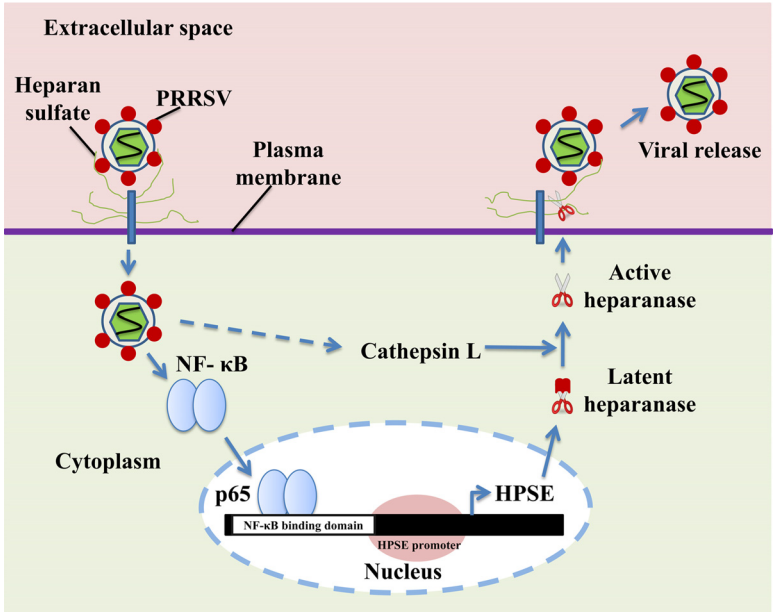

FIG 7 Schematic model of PRRSV release. During the productive period of infection, PRRSV activates NF-κB to promote HPSE mRNA transcription, thus increasing heparanase expression. Simultaneously, PRRSV activates the proteolytic activity of cathepsin L, which subsequently processes latent heparanase into its enzymatically active form. The active heparanase is then translocated to the cell surface and exerts enzymatic activity to cleave HS of the ECM, resulting in the release of virus attached to fragments of ECM-resident HS.

L to upregulate and process heparanase; then the active heparanase cleaved HS, which is beneficial for viral release. To avoid being trapped by parent host cells during influenza virus release, neuraminidase, which is encoded by the virus, can destroy the hemagglutinin receptor on the host cell, thus allowing release of progeny virus particles from infected cells (34). However, until now, PRRSV was not known to produce any enzymes in its genome that are capable of cleaving HS. In the current study, we demonstrated that PRRSV activated a host-derived enzyme, namely, heparanase, to degrade HS during the virus life cycle (Fig. 1 and 2). Since HS is used by many viruses for initial attachment to target cells, it is reasonable to assume that heparanase might be involved in the pathogenesis of other viruses as well. It has been reported that dengue virus nonstructural protein 1 (NS1) disrupts the endothelial glycocalyx layer on human pulmonary microvascular endothelial cells by NS1-induced expression of sialidases and heparanase (23). Furthermore, heparanase is upregulated in numerous human diseases such as cancer, diabetes, renal disease, and Alzheimer's disease (35, 36).

In conclusion, our findings reveal for the first time that heparanase, an HS-degrading enzyme of the host, is involved in regulation of PRRSV release. Therefore, targeting the activity of heparanase might be an excellent candidate for the development of future antiviral strategies against PRRSV infection. In addition, our results provide new insight into the molecular mechanism of PRRSV egress from host cells (Fig. 7), which might help us to further understand PRRSV pathogenesis.

MATERIALS AND METHODS

Cells and viruses. Porcine alveolar macrophages (PAMs) were obtained from lung lavage samples from the lungs of 3- to 8-week-old PRRSV-negative piglets (37, 38) and cultured in RPMI 1640 medium supplemented with 10% heat-inactivated fetal bovine serum (FBS; PAA, Pasching, Austria), 100 U/ml penicillin, and 100 μg/ml streptomycin sulfate at 37°C in 5% CO_2. All animal experiments were approved by the Institutional Animal Care and Use Committee of Sun Yat-sen University. Marc-145 cells were cultured in Dulbecco's modified Eagle's medium (DMEM; Sigma, St. Louis, MO, USA) containing 10% FBS. Viruses used in this study were a classical North American type PRRSV, strain CH-1a (GenBank accession number AY032626.1), kindly provided by Guihong Zhang of South China Agricultural University, and a

TABLE 1 The sequences of primers used in this study

Primer group and name[a]	Sequence (5′–3′)
Primers for qRT-PCR	
GAPDH-F	TGACAACAGCCTCAAGATCG
GAPDH-R	GTCTTCTGGGTGGCAGT GA
p65-F	TGGGGACTACGACCTGAATG
p65-R	GGGGGCACGATTGTCAAAGA
HS-F	CCTGACGGCCACTTCTACC
HS-R	GCAGGCATCACCACATTCAC
Heparanase-F1	AACCATAGACGGCAACCTGG
Heparanase-R1	TCTCAGGTATGCGGGAGACA
Cathepsin L-F	GCTGGTGGTTGGCTATGGAT
Cathepsin L-R	GCGGAGGCAATTCCACAATG
Primers for the heparanase gene	
Heparanase-F2	ATGGAGGGCGCAGTGGG
Heparanase-R2	TCAGATGCAAGCAGCAACTTT

[a]F, forward primer, R, reverse primer.

recombinant PRRSV. The recombinant PRRSV, a kind gift from Shuqi Xiao of Northwest A&F University, China, can express enhanced green fluorescent protein (EGFP) as a specific marker (designated PRRSV-EGFP).

qRT-PCR. Total RNA was isolated from Marc-145 cells or PAMs using TRIzol reagent (Invitrogen, CA, USA) and reverse transcribed using a PrimeScript RT reagent kit (TaKaRa, Dalian, China) in accordance with the manufacturer's instructions. SYBR green (TaKaRa, Osaka, Japan) real-time PCR was performed using a Light-Cycler 480 PCR system (Roche, Basel, Switzerland). Reactions were performed in a 10-μl volume. Relative quantities of mRNA accumulation were evaluated using the $2^{-\Delta CT}$ (where C_T is threshold cycle) method. The primers used for real-time quantitative reverse-transcription PCR (qRT-PCR) are listed in Table 1.

IFA. An immunofluorescence assay (IFA) was performed as previously described (39) with modifications. Cells were seeded onto coverslips and then fixed with 4% paraformaldehyde and permeabilized with 0.5% Triton X-100 at room temperature (RT). After being incubated for the 30 min, cells were rinsed with phosphate-buffered saline (PBS) three times and blocked with 1% bovine serum albumin (BSA) in PBS for 30 min at RT and then incubated overnight with anti-human HS MAb 10E4 (1:200; US Biological, MA, USA) or anti-NF-κB p65 MAb (1:200; Cell Signal Technology, MA, USA) at 4°C. After being washed with PBS, cells were further incubated with Alexa Fluor 555-conjugated anti-mouse IgG secondary antibody (1:200; Cell Signal Technology) for 2 h at RT. Cell nuclei were stained with 4′,6′-diamidino-2-phenylindole (DAPI; 1 μg/ml [Beyotime, China]) and detected using fluorescence microscopy (Carl Zeiss, Jena, Germany).

Western blot analysis. For Western blot experiments, the primary antibodies anti-PRRSV N protein MAb (1:2,000; Jeno Biotech, Inc., Republic of Korea), anti-heparanase MAb (1:1,000; Abcam), anti-NF-κB p-IκBα MAb (1:2,000; Cell Signal Technology), anti-cathepsin L (1:1,000; Abcam), anti-glyceraldehyde phosphate dehydrogenase (GAPDH) MAb (1:2,000; Cell Signal Technology), horseradish peroxidase-conjugated anti-mouse IgG antibody, and anti-rabbit IgG antibody (1:2,000; Cell Signal Technology) were used. Marc-145 cells or PAMs cultured in six-well plates were harvested in lysis buffer (Beyotime, Jiangsu, China) containing a cocktail of protease inhibitors (Roche). The cell extracts were boiled in SDS protein sample buffer and then resolved by 12% SDS-PAGE. The separated proteins were transferred to polyvinylidene difluoride (PVDF) membranes (Millipore, MA, USA). After the membranes were blocked with 5% nonfat dry milk in TBST (20 mM Tris [pH 7.5], 150 mM NaCl, 0.5% Tween 20) for 2 h at 37°C, they were rinsed and incubated with the antibody indicated on the figures. Protein bands were visualized with ECL Plus chemiluminescence reagent (Pierce, Rockford, USA).

PRRSV titration assay. In order to analyze the growth of PRRSV, the viral supernatants from cell cultures were collected at the time points after virus infection indicated on the figures. Virus titers were expressed as the 50% tissue culture infective dose ($TCID_{50}$) per 0.1 ml using the Reed-Muench method. Briefly, Marc-145 cells were seeded at a density of 4.0×10^5 cells/ml culture medium in each well of 96-well plates before virus infection. Viral supernatants were prepared by 10-fold serial dilution, and 100 μl of the dilutions was added per well in eight replicates. Virus titers were calculated at 4 to 5 days postinfection.

Enzymatic activity assay. Cathepsin L activity in living cells was monitored using a Magic Red cathepsin L detection kit (ImmunoChemistry Technologies, MN, USA). Briefly, cells were seeded onto coverslips and then inoculated with PRRSV at a multiplicity of infection (MOI) of 1, 2, or 3. After incubation for the times indicated on the figures, Magic Red staining solution, which is a noncytotoxic substrate that fluoresces red upon cleavage by active cathepsins, was added for 1 h at 37°C. Cells were detected using a fluorescence microscope equipped with an excitation filter of 550 nm (540 to 560 nm) and a long-pass >610-nm emission filter pair.

siRNA knockdown. The siRNAs targeting heparanase were synthesized by Ribobio (Guangzhou, China). Transient transfection of siRNA was performed using Lipofectamine RNAiMAX transfection reagent (Invitrogen, CA, USA) according to the manufacturer's protocol. Briefly, Marc-145 cells were

TABLE 2 The sequences of siRNAs used in this study

Heparanase siRNA	Sequence (5′–3′)	
	Sense	Antisense
S1	CAGUUGCUGCUGGACUACUGCUCUU	AAGAGCAGUAGUCCAGCAGCAACUG
S2	UAUCCAGCCACAUAAAGCCAGCUGC	GCAGCUGGCUUUAUGUGGCUGGAUA
S3	GAAGUUCACUGGGCUUGCCAGCUUU	AAAGCUGGCAAGCCCAGUGAACUUC
NC	UUCUCCGAACGUGUCACGUTTAUUA	ACGUGACACGUUCGGAGAATTUAGG

cultured in six-well plates to 70% confluence and then transfected with different final concentrations of siRNAs. At 48 h posttransfection, cells were collected for qRT-PCR or Western blot analysis to evaluate the efficiency of knockdown. The siRNAs are listed in Table 2.

Heparanase overexpression. To construct a heparanase overexpression vector, the heparanase coding sequence was amplified by PCR using the primers listed in Table 1 and then cloned into NheI and XhoI sites in a pcDNA3.1(+) vector (Invitrogen, CA, USA) to produce pcDNA3.1-heparanase. Marc-145 cells were transfected with pcDNA3.1-heparanase or a control vector using Lipofectamine 3000 (Invitrogen, CA, USA) according to the manufacturer's instructions. The dose of pcDNA3.1-heparanase (1.5 μg/ml) used for transfection was optimized in the experiments, and no appreciable cellular toxicity was observed.

Flow cytometry. HS cell surface expression was examined after PRRSV-EGFP infection. Cells were suspended in PBS at a concentration of 1×10^6 cells/ml and incubated with mouse anti-human HS MAb 10E4 diluted in PBS with 1% BSA (1:100; US Biological, MA, USA) for 1 h at 4°C. After being washed with PBS, cells were further incubated with Alexa Fluor 555-conjugated anti-mouse IgG secondary antibody (1:200; Cell Signal Technology) for 45 min at 4°C. PRRSV-EGFP-positive cells were also detected by flow cytometry. Typically, 10,000 labeled cells were acquired using a FACSCalibur (BD Bioscience, CA, USA) and analyzed using FlowJo, version 8.7, software.

Statistical analysis. All experiments were performed with at least three independent replicates. All data are presented as means ± standard errors (SE). Statistical analysis was performed by SPSS, version 16.0, using Student's *t* test and one-way analysis of variance (ANOVA). Differences with P values of <0.05 were considered significant. The results were analyzed using Student's *t* test if two groups were compared and using one-way analysis of variance if more groups were tested against a control group.

ACKNOWLEDGMENTS

This work was supported by the National Natural Science Foundation of China (31601917), Natural Science Foundation of Guangdong Province (2014A030312011), and Science and Technology Planning Project of Guangzhou (201607020014).

Chunhe Guo conceived and designed the study. Chunhe Guo, Zhenbang Zhu, and Yang Guo performed the experiments, analyzed the data, and drafted the manuscript. Chunhe Guo, Zhenbang Zhu, Yang Guo, Xiaoying Wang, Piao Yu, Shuqi Xiao, Yaosheng Chen, Yongchang Cao, and Xiaohong Liu coordinated the study. Zhenbang Zhu and Yaosheng Chen contributed to the interpretation of the data and took part in critical revisions of the manuscript.

We declare that we have no competing interests.

REFERENCES

1. Pileri E, Mateu E. 2016. Review on the transmission porcine reproductive and respiratory syndrome virus between pigs and farms and impact on vaccination. Vet Res 47:108. https://doi.org/10.1186/s13567-016-0391-4.
2. Guo C, Chen L, Mo D, Chen Y, Liu X. 2015. DRACO inhibits porcine reproductive and respiratory syndrome virus replication in vitro. Arch Virol 160:1239–1247. https://doi.org/10.1007/s00705-015-2392-4.
3. Li N, Du T, Yan Y, Zhang A, Gao J, Hou G, Xiao S, Zhou EM. 2016. MicroRNA let-7f-5p inhibits porcine reproductive and respiratory syndrome virus by targeting MYH9. Sci Rep 6:34332. https://doi.org/10.1038/srep34332.
4. Liu X, Guo C, Huang Y, Zhang X, Chen Y. 2015. Inhibition of porcine reproductive and respiratory syndrome virus by Cecropin D in vitro. Infect Genet Evol 34:7–16. https://doi.org/10.1016/j.meegid.2015.06.021.
5. Chen J, Shi X, Zhang X, Wang A, Wang L, Yang Y, Deng R, Zhang GP. 2017. MicroRNA 373 facilitates the replication of porcine reproductive and respiratory syndrome virus by its negative regulation of type I interferon induction. J Virol 91:e01311–16. https://doi.org/10.1128/JVI.01311-16.
6. Wang X, Yang X, Zhou R, Zhou L, Ge X, Guo X, Yang H. 2016. Genomic characterization and pathogenicity of a strain of type 1 porcine reproductive and respiratory syndrome virus. Virus Res 225:40–49. https://doi.org/10.1016/j.virusres.2016.09.006.
7. Zhang M, Li X, Deng Z, Chen Z, Liu Y, Gao Y, Wu W. 2017. Structural biology of the arterivirus nsp11 endoribonucleases. J Virol 91:e01309–16. https://doi.org/10.1128/JVI.01309-16.
8. Bai X, Wang Y, Xu X, Sun Z, Xiao Y, Ji G, Li Y, Tan F, Li X, Tian K. 2016. Commercial vaccines provide limited protection to NADC30-like PRRSV infection. Vaccine 34:5540–5545. https://doi.org/10.1016/j.vaccine.2016.09.048.
9. Tian K, Yu X, Zhao T, Feng Y, Cao Z, Wang C, Hu Y, Chen X, Hu D, Tian X, Liu D, Zhang S, Deng X, Ding Y, Yang L, Zhang Y, Xiao H, Qiao M, Wang B, Hou L, Wang X, Yang X, Kang L, Sun M, Jin P, Wang S, Kitamura Y, Yan J, Gao GF. 2007. Emergence of fatal PRRSV variants: unparalleled outbreaks of atypical PRRS in China and molecular dissection of the unique hallmark. PLoS One 2:e526. https://doi.org/10.1371/journal.pone.0000526.
10. Fablet C, Marois-Crehan C, Grasland B, Simon G, Rose N. 2016. Factors associated with herd-level PRRSV infection and age-time to seroconversion in farrow-to-finish herds. Vet Microbiol 192:10–20. https://doi.org/10.1016/j.vetmic.2016.06.006.
11. Jeong J, Choi K, Kang I, Park C, Chae C. 2016. Evaluation of a 20 year old

porcine reproductive and respiratory syndrome (PRRS) modified live vaccine (Ingelvac® PRRS MLV) against two recent type 2 PRRS virus isolates in South Korea. Vet Microbiol 192:102–109. https://doi.org/10.1016/j.vetmic.2016.07.006.
12. Zhang L, Cui Z, Zhou L, Kang Y, Li L, Li J, Dai Y, Yu S, Li N. 2016. Developing a triple transgenic cell line for high-efficiency porcine reproductive and respiratory syndrome virus infection. PLoS One 11: e0154238. https://doi.org/10.1371/journal.pone.0154238.
13. Van Breedam W, Van Gorp H, Zhang JQ, Crocker PR, Delputte PL, Nauwynck HJ. 2010. The M/GP(5) glycoprotein complex of porcine reproductive and respiratory syndrome virus binds the sialoadhesin receptor in a sialic acid-dependent manner. PLoS Pathog 6:e1000730. https://doi.org/10.1371/journal.ppat.1000730.
14. Zhang Q, Yoo D. 2015. PRRS virus receptors and their role for pathogenesis. Vet Microbiol 177:229–241. https://doi.org/10.1016/j.vetmic.2015.04.002.
15. Goodall KJ, Poon IK, Phipps S, Hulett MD. 2014. Soluble heparan sulfate fragments generated by heparanase trigger the release of pro-inflammatory cytokines through TLR-4. PLoS One 9:e109596. https://doi.org/10.1371/journal.pone.0109596.
16. Rivara S, Milazzo FM, Giannini G. 2016. Heparanase: a rainbow pharmacological target associated to multiple pathologies including rare diseases. Future Med Chem 8:647–680. https://doi.org/10.4155/fmc-2016-0012.
17. Yang Y, Gorzelanny C, Bauer AT, Halter N, Komljenovic D, Bauerle T, Borsig L, Roblek M, Schneider SW. 2015. Nuclear heparanase-1 activity suppresses melanoma progression via its DNA-binding affinity. Oncogene 34:5832–5842. https://doi.org/10.1038/onc.2015.40.
18. Hadigal SR, Agelidis AM, Karasneh GA, Antoine TE, Yakoub AM, Ramani VC, Djalilian AR, Sanderson RD, Shukla D. 2015. Heparanase is a host enzyme required for herpes simplex virus-1 release from cells. Nat Commun 6:6985. https://doi.org/10.1038/ncomms7985.
19. Wu W, Pan C, Yu H, Gong H, Wang Y. 2008. Heparanase expression in gallbladder carcinoma and its correlation to prognosis. J Gastroenterol Hepatol 23:491–497. https://doi.org/10.1111/j.1440-1746.2007.04945.x.
20. Wu W, Pan C, Meng K, Zhao L, Du L, Liu Q, Lin R. 2010. Hypoxia activates heparanase expression in an NF-κB dependent manner. Oncol Rep 23:255–261. https://doi.org/10.3892/or_00000797.
21. Zhang Q, Huang C, Yang Q, Gao L, Liu HC, Tang J, Feng WH. 2016. MicroRNA-30c modulates type I IFN responses to facilitate porcine reproductive and respiratory syndrome virus infection by targeting JAK1. J Immunol 196:2272–2282. https://doi.org/10.4049/jimmunol.1502006.
22. Fu Y, Quan R, Zhang H, Hou J, Tang J, Feng WH. 2012. Porcine reproductive and respiratory syndrome virus induces interleukin-15 through the NF-κB signaling pathway. J Virol 86:7625–7636. https://doi.org/10.1128/JVI.00177-12.
23. Puerta-Guardo H, Glasner DR, Harris E. 2016. Dengue virus NS1 disrupts the endothelial glycocalyx, leading to hyperpermeability. PLoS Pathog 12:e1005738. https://doi.org/10.1371/journal.ppat.1005738.
24. Abboud-Jarrous G, Atzmon R, Peretz T, Palermo C, Gadea BB, Joyce JA, Vlodavsky I. 2008. Cathepsin L is responsible for processing and activation of proheparanase through multiple cleavages of a linker segment. J Biol Chem 283:18167–18176. https://doi.org/10.1074/jbc.M801327200.
25. Shteingauz A, Ilan N, Vlodavsky I. 2014. Processing of heparanase is mediated by syndecan-1 cytoplasmic domain and involves syntenin and alpha-actinin. Cell Mol Life Sci 71:4457–4470. https://doi.org/10.1007/s00018-014-1629-9.
26. Bacsa S, Karasneh G, Dosa S, Liu JA, Valyi-Nagy T, Shukla D. 2011. Syndecan-1 and syndecan-2 play key roles in herpes simplex virus type-1 infection. J Gen Virol 92:733–743. https://doi.org/10.1099/vir.0.027052-0.
27. Hao NB, Tang B, Wang GZ, Xie R, Hu CJ, Wang SM, Wu YY, Liu E, Xie X, Yang SM. 2015. Hepatocyte growth factor (HGF) upregulates heparanase expression via the PI3K/Akt/NF-κB signaling pathway for gastric cancer metastasis. Cancer Lett 361:57–66. https://doi.org/10.1016/j.canlet.2015.02.043.
28. Goldberg R, Rubinstein AM, Gil N, Hermano E, Li JP, van der Vlag J, Atzmon R, Meirovitz A, Elkin M. 2014. Role of heparanase-driven inflammatory cascade in pathogenesis of diabetic nephropathy. Diabetes 63: 4302–4313. https://doi.org/10.2337/db14-0001.
29. Jung O, Trapp-Stamborski V, Purushothaman A, Jin H, Wang H, Sanderson RD, Rapraeger AC. 2016. Heparanase-induced shedding of syndecan-1/CD138 in myeloma and endothelial cells activates VEGFR2 and an invasive phenotype: prevention by novel synstatins. Oncogenesis 5:e202. https://doi.org/10.1038/oncsis.2016.5.
30. Cui H, Tan YX, Osterholm C, Zhang X, Hedin U, Vlodavsky I, Li JP. 2016. Heparanase expression upregulates platelet adhesion activity and thrombogenicity. Oncotarget 7:39486–39496.
31. Liu XY, Tang QS, Chen HC, Jiang XL, Fang H. 2013. Lentiviral miR30-based RNA interference against heparanase suppresses melanoma metastasis with lower liver and lung toxicity. Int J Biol Sci 9:564–577. https://doi.org/10.7150/ijbs.5425.
32. Wang D, Fan J, Fang L, Luo R, Ouyang H, Ouyang C, Zhang H, Chen H, Li K, Xiao S. 2015. The nonstructural protein 11 of porcine reproductive and respiratory syndrome virus inhibits NF-κB signaling by means of its deubiquitinating activity. Mol Immunol 68:357–366. https://doi.org/10.1016/j.molimm.2015.08.011.
33. Jing H, Fang L, Ding Z, Wang D, Hao W, Gao L, Ke W, Chen H, Xiao S. 2017. Porcine reproductive and respiratory syndrome virus nsp1α inhibits NF-κB activation by targeting the linear ubiquitin chain assembly complex. J Virol 91:e01911–16. https://doi.org/10.1128/JVI.01911-16.
34. Air GM, Laver WG. 1989. The neuraminidase of influenza virus. Proteins 6:341–356. https://doi.org/10.1002/prot.340060402.
35. Yang Y, Ren YS, Ramani VC, Nan L, Suva LJ, Sanderson RD. 2010. Heparanase enhances local and systemic osteolysis in multiple myeloma by upregulating the expression and secretion of RANKL. Cancer Res 70:8329–8338. https://doi.org/10.1158/0008-5472.CAN-10-2179.
36. Goldberg R, Meirovitz A, Hirshoren N, Bulvik R, Binder A, Rubinstein AM, Elkin M. 2013. Versatile role of heparanase in inflammation. Matrix Biol 32:234–240. https://doi.org/10.1016/j.matbio.2013.02.008.
37. Guo C, Cong P, He Z, Mo D, Zhang W, Chen Y, Liu X. 2015. Inhibitory activity and molecular mechanism of protegrin-1 against porcine reproductive and respiratory syndrome virus in vitro. Antivir Ther 20:573–582. https://doi.org/10.3851/IMP2918.
38. Guo C, Huang Y, Cong P, Liu X, Chen Y, He Z. 2014. Cecropin P1 inhibits porcine reproductive and respiratory syndrome virus by blocking attachment. BMC Microbiol 14:273. https://doi.org/10.1186/s12866-014-0273-8.
39. Zhang A, Zhao L, Li N, Duan H, Liu H, Pu F, Zhang G, Zhou EM, Xiao S. 2017. Carbon monoxide inhibits porcine reproductive and respiratory syndrome virus replication by the cyclic GMP/protein kinase G and NF-κB signaling pathway. J Virol 91:e01866–16. https://doi.org/10.1128/JVI.01866-16.